Investigating a Recalibration Mechanism of a Path Integration Model

Ayoub EL HOUDRI

Department of Computer Science
CY Cergy Paris University and ENSEA
95014 Cergy-Pontoise, France
ayoub.elhoudri@ensea.fr

Abstract—**Accurate navigation and memory formation in dynamic environments require a continuous real-time update of spatial representations. This adaptive process, known as remapping, plays a crucial role in achieving precision in navigation tasks within continuously changing environments. In this article, we use a model that employs a path integration (PI) mechanism derived from neural head direction (HD) cells modulated by the linear speed of the animal. We introduce a mechanism for recalibrating PI through visual place cells (VPC) generated from visual information surrounding the animal. Our objective is to present and analyze the capabilities and limitations of our PI recalibration mechanism and investigate through an experiment how PCs, generated by the model, respond to environmental changes.**

Keywords—**Navigation, Place Cells, Path Integration, Remapping**

I. INTRODUCTION

The discovery of PCs and their role in spatial navigation has been a breakthrough in the field of neuroscience [1]. Place cells are neurons that exhibit selective firing patterns when an animal occupies a particular location in its environment. The firing pattern of these cells forms a place code of the navigated environment allowing the animal to orient itself and remember spatial information.

Several studies have shown that the brain can integrate multiple sources of information to update its internal representation of space [2]: PCs are especially influenced by both external visual cues, such as landmarks [3], [4], and internal cues, such as self-motion [5], [6].

Numerous studies have examined the impact of visual and idiothetic cues on the activity of PCs as well as the hierarchy between them [7]. The findings have been inconsistent. Some studies suggest that visual cues are more influential than idiothetic cues [8], while others suggest the opposite [9]. Other studies show mixed results, depending on the specific conditions of the experiment [10]. For instance, under particular experimental circumstances, rodents predominantly rely on the PI mechanism for navigation, a concept introduced in [11]. Only after repeated attempts do rodents begin to use the present landmarks to direct their navigation [12].

Another important aspect of PCs is their ability to show a remapping. Remapping in the context of navigation refers to the phenomenon in which the firing patterns of PCs change in response to changes in the environment [1]. This means that the same location in different environments can be represented by different groups of place cells. Remapping is thought to be important for allowing animals to distinguish between different environments and prevent confusion between similar environments [13].

Remapping has been observed in a variety of contexts, including changes in visual landmarks, alterations in the shape or size of the environment, and changes in the lighting or odor of the environment [13], [14]. Interestingly, remapping is not limited to the hippocampus, as other brain regions, such as the entorhinal cortex (EC), have also been shown to exhibit remapping [15]. This suggests that remapping is a general feature of neural circuits involved in spatial navigation.

Previous studies employing PCs generated solely from self-motion have demonstrated that animals utilize path integration PI to differentiate visually identical compartments based on changes in their spatial representations. For example, partial remapping was observed in [16], while [17] noted nearly complete remapping. These findings highlight the significance of PI in the process of updating spatial representations of space. In support of this, our model incorporates PI to generate PC-like activity. Additionally, a mechanism for recalibrating PI through vision is introduced to ensure the stability of these PCs over time.

In this article, we will present the architecture of our model, encompassing the encoding of visual information, the mechanism for generating PC-like activity from an approximation of the PI, and the design of our PI recalibration mechanism. We will provide an analysis of its capabilities, including adaptability to changes in the environment, as well as discuss its limitations and potential avenues for improvement.

II. MODEL

Our computational model comprises three populations of neurons, as illustrated in Fig. 2. The first population consists of VPCs associated with visual information, created using the PerAc architecture [18]. They learn the place code of the navigated environment from a constellation of different landmarks. The second population is a group of neurons encoding PI. This population is formed through an approximation of the PI mechanism, by integrating a neural field of HD modulated by
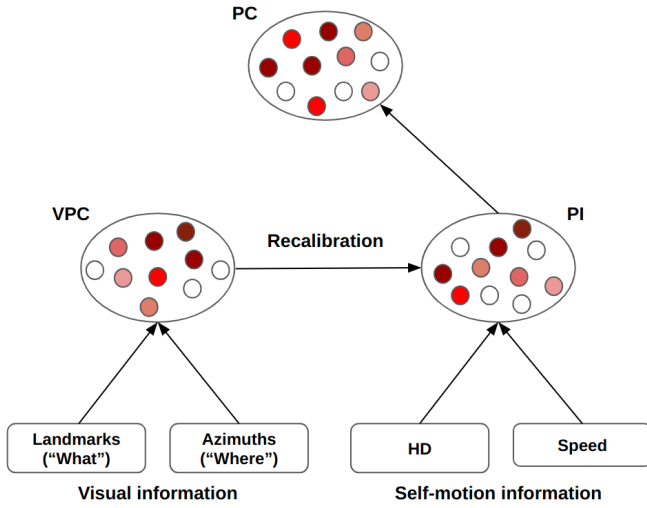
Fig. 1. Schematic representation of our model. The figure shows three populations of interconnected neurons: VPC, built from visual landmarks and azimuth, and PI neurons, built from HD and speed of the agent. VPC is used to calibrate PI and generate a robust PC population.

speed. The last population is a group of cells with a PC-like activity that we will call PCs, created through a straightforward model introduced in [19], resulting from a PI corrected by vision.

The recursive nature of PI leads to error accumulation after navigating for a long time in the environment without returning to the starting point, this limitation is discussed in [20]. Without a corrective mechanism, a breakdown in the calculation of location can occur [21].

Taking into account the behavioral evidence of PI being corrected using visual information [22]–[24], we implemented a PI recalibration mechanism relying on vision.

A. Visual Place Cells Model
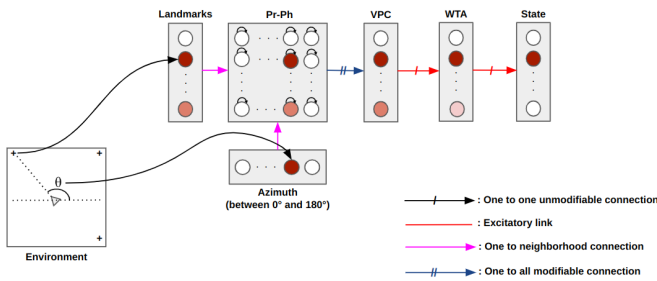
Fig. 2. The figure shows the architecture of the model used to create VPCs through the Pr-Ph for the "what" (Landmarks) and "where" (Azimuth) information, followed by a WTA to select only one neuron, called state, to code a single place

The VPC model (Fig. 2) is a neural network that processes a local view of a 2D environment containing landmarks to extract and recognize constellations of these landmarks as well as their identity. By merging "What" (landmark) and

"Where" (azimuth) information in the perirhinal and post-rhinal cortices, as claimed in [25], corresponding to the Pr-Ph structure in our model, the model can activate a neuron in the Pr-Ph structure only when a local view is recognized under a specific azimuth. This mechanism enables a VPC to construct a global code for the current location with a dynamic short-term memory to create a sufficiently wide place field, to avoid confusion between places that can occur when dealing with a discrete environment, and to ensure continuity of place encoding in the environment. Additionally, a competitive mechanism is used to select the winning neuron that best recognizes the current place. A detailed explanation of the model as well as the equations behind the model are given in [26], [27].

The activity of VPCs corresponds to the level of recognition of landmarks under a given azimuth. To ensure the firing of one neuron for each recognized place, a Winner-Takes-All (WTA) mechanism [28] establishes competition between VPCs. The one with the highest activation level ends by encoding the current place.

This model has demonstrated robustness in generating a spatial map of the environment from visual input. Different robotics experiments using the VPC model validate its robust performance [27], [29], [30].

B. Path Integration Model
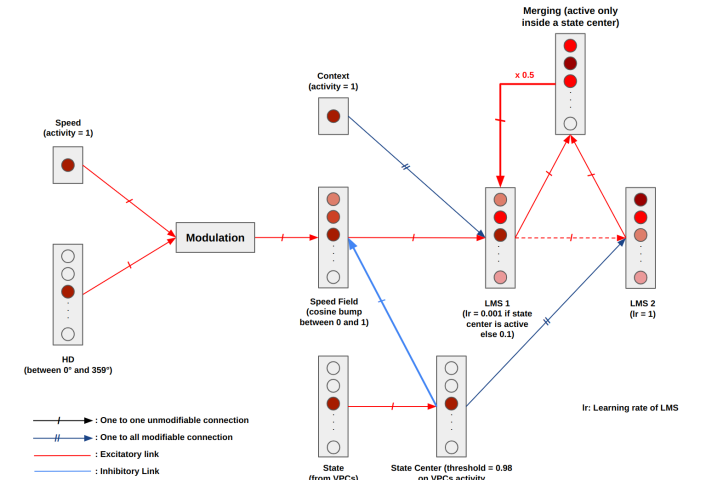
Fig. 3. The figure illustrates the model employed for learning PI. This is achieved through LMS1 learning from HD modulated by the linear speed of the animal with a learning rate of 0.001. A vision-based recalibration is shown through a loop, which is effective only when a state center is active. In this loop, LMS2 learns the association between well-known visual places and the one time step delayed PI with a learning rate of 1. Subsequently, the learned signal is added to LMS1's previous output signal. To prevent saturation, the output is divided by two and then directly used to be learned by LMS1 with a recalibration learning rate of 0.1. The loop concludes only when the state center is no longer active.

The base model used here aims to generate neurons with a PC-like activity from a field of PI neurons constructed from HD information modulated by the speed of the animal [32].

The model is based on the work presented in [33] and is further studied in different experimental setups in [19], [30].

The architecture of the model is simplified by creating a so-called "speed field" that incorporates only discretized HD with an activity corresponding to the speed of the animal, and where each neuron of the field corresponds to a discrete heading direction in the environment. We suppose that the head direction of the animal is the same as the direction of movement of the animal. We use a positive cosine bump, as presented in Eq. 1 and as shown in Fig. 4, exhibiting activation values between 0 and 1 and reaching its maximum at the current heading direction θ_i. A Gaussian bump with a carefully chosen standard deviation can be used to approximate the cosine, for biological plausibility, as shown in [34]. We chose a positive cosine function which is more suitable for a stable PI [20].

$$U_i(\Phi(t)) = (1 + \cos(\Phi(t) - \theta_i))/2 \qquad (1)$$
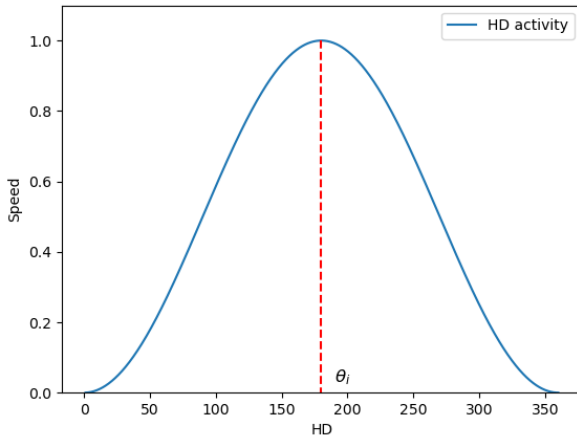
Fig. 4. The figure shows the shape of the speed field at time t, encoded on a 360 HD neuron modulated by the speed of the animal. The heading direction is $\theta(t)$

In our simulations, we use N neurons to encode the speed field. We chose $N = 360$ to encode HD information, resulting in $\theta_i = -2\pi \frac{i}{360}$ HD possible angles, where $i \in \{0, \ldots, 359\}$. A large discretization step of the HD field can lead to a lack of precision for PI encoded also on the same number of neurons N, which leads to angular error propagation by missing the precise value of some angles [20]. The higher is N, the better the precision; for our model, we consider setting $N = 360$ sufficiently appropriate to avoid error accumulation [20].

The speed field is then learned through classical conditioning relying on the Least Mean Squares (LMS) learning rule [31] and performing the same task as a short-term memory (STM). The mathematical proof of the LMS approximating the mechanism of PI and the equivalence between LMS and STM is highlighted in equation (5) in the appendix.

To construct a spatial code for the navigated environment based on PI, we follow the procedure outlined in [19]. We derive PC-like activity through the discretization of neuron activity within the PI field. This involves subtracting the average activity value of all neurons in the PI field, resulting in a field of PI comprising both positive and negative "activities" referred to as the vector integration field (VIF). Simultaneously, the positive and negative activities are projected into a Kohonen self-organizing map [36], producing neurons exhibiting PC-like activity. Each neuron is then selected and attributed to one specific location through a winner-takes-all (WTA) process. We will call these cells "place cells" (PCs), and they represent a spatial code of the environment. These neurons are the focal point for our investigation of the phenomenon of remapping.

C. Recalibration mechanism

Since PI tends to accumulate errors during animal travels without returning to the starting point within a reasonable time or during high-angular-speed turns, various methods are used to correct it. Some involve simply resetting PI to zero after error accumulation, achieved by visually detecting the starting point through the first active VPC, often facilitated by periodic homing. When the first learned VPC with a place field corresponding to the starting point is recognized, an inhibition process resets the PI neurons [30]. Another solution involves using a binary signal; when a VPC exhibits very high activity, the binary signal is triggered [20] to set the PI field activity to zero in one shot. These methods prevent error accumulation and were tested in different robotics experiments, such as in [30].

Another method consists of achieving a reset of PI by identifying novelty, as discussed in previous studies [?], [?]. Specifically, the PI reset is triggered when the novelty gradient becomes null.

A more plausible alternative consists of recalibrating PI without resetting it to zero. This method is very similar to our recalibration mechanism that will be presented next. As used in [30] and in a slightly different way in [37], this approach involves learning to associate the PI field with the winning VPC each time through an LMS algorithm. This allows the system to recalibrate PI when places are well visually recognized: specifically, when the activity of the most active VPC exceeds a static threshold, along with a significant difference in activity between the two most consecutively active VPCs.

Our recalibration mechanism, shown in the model architecture in Fig. 3, comprises two consecutive LMS algorithms. The first, LMS1, directly performs PI from the speed field by learning the association between a context with constant activity set to 1 and the speed field. Meanwhile, LMS2 performs one-shot learning, associating PI with the center of each state. When the agent is in a state center, LMS2 rapidly adapts its weights to approximate the PI arriving with a very small delay. The learned PI and the current PI are

then merged, to be learned again by LMS1 more rapidly than usual. This process is a replacement for the previous PI with the new one that takes into account visual information, and this process continues until the animal exits the center of the state, indicating insufficient place recognition. The theoretical details of the recalibration loop functioning can be found in the appendix.

The state center is derived from VPCs, selecting only those with activity above a threshold of 0.98 to ensure recalibration in particular areas. This approach ensures that the association is learned only when a state-center neuron is active, at the center of each place field. This strategy prevents recalibrating PI in confusing locations, as explained in [30].

III. SIMULATIONS
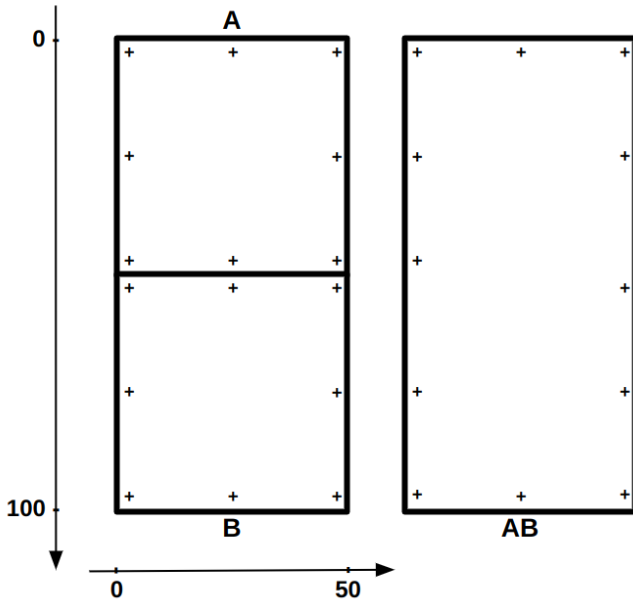
Fig. 5. The figure shows room A, room B, and room AB the merging of room A and B. Each symbol "+" represents a landmark with a unique identity

The animal is simulated according to its (x, y) coordinates, taking a constant speed and a randomly chosen head direction (HD) at each time step without significant changes. This approach aims to prevent the agent from drifting and to generate a plausible movement pattern.

Our experiment is similar to the one in [38], [39]. It involves exploring a first square room, A, with various landmarks, followed by a second square room, B, which also contains the same number of landmarks. These landmarks are positioned near the boundaries of the rooms, as shown in Fig. 5. After constructing separate spatial codes for each room, the boundary separating the two rooms is removed to enable the agent to explore the new room AB, resulting from the merging of room A and room B. In this combined room, only 12 out of the initially set 16 landmarks for rooms A and B are retained. This adjustment is made to ensure that some previously active

VPCs in both rooms also remain active in the new, merged room. The environment parameters for each room are in Table. I. We expand the recalibration area for each place field since the activity of the VPCs depends on the recognition level of landmarks, which varies between rooms A, B, and the new one AB.

Our goal is to have the agent learn a stable place code through the PCs recruited in rooms A and B. When switching to room AB, we cease the recruitment of new VPCs and observe the dynamics of the PCs over time, monitoring how the change of their firing patterns in the new environment.

We set the learning rate of the LMS1 outside recalibration zones to be 0.001, which correctly approximates the process of PI in an environment of size 2m $\times$ 2m, as shown in [19].

In our model, we attempted to determine the recalibration parameters that contribute to achieving the optimal stability of the place cells (PCs), which is still a hard task, due to the high sensitivity of our model to these parameters. Consequently, we established the recalibration learning rate of LMS1 as 0.1. The learning rate of LMS2 remains constant and is set to 1. Within a recalibration zone, the merging of LMS1 and LMS2 outputs occurs, and the result is divided by two to maintain the same scale as the previous PI homing vector, knowing that LMS2 approximates LMS1 output in one-shot learning.

We ran the simulation, initially starting in room A at the origin $(10, 10)$ for a duration of 80000 time-steps. Subsequently, we moved the animal to point $(40, 90)$ for another duration of 80000 time-steps. Following this, the separating wall between room A and room B was removed to allow the animal to navigate the new environment AB. In this combined space, there is no learning of new place VPCs or PCs. We rely solely on what has been learned in the two rooms separately, and the navigation lasts for 180000 time-steps. The parameters used for the simulation in rooms A and B, and then in room AB, are detailed in Appendix II and III respectively.

TABLE I
ENVIRONMENT PARAMETERS

Parameters	Room A	Room B	Room AB
Environment size	2 m × 2m	2 m × 2m	2 m × 4m
Number of landmarks	8 landmarks	8 landmarks	12 landmarks

IV. RESULTS

We recorded the activity of PCs as the agent navigated each room. From this recording, we examined the place fields of the PCs during the last 20000 time-steps for rooms A and B, during which the place field of each cell was sufficiently stable. For room AB, we monitored the place fields of the same cells, observing their evolution and activity during each 40000 time-step segment throughout the entire 180000 time-steps.

We observe that the place field centers, representing the maximum activity, have shifted slightly in the new room AB compared to their positions in room B, for PC 51 and PC 43, as shown in Figures 6 and 7. This indicates that

the PCs are attempting to adapt to the new environment. However, since the experiment was conducted in room AB for only a duration of 180000 time-steps, we cannot conclusively determine whether a complete remapping has occurred. The duration may be insufficient for establishing a very stable place code, and this is due to the limitations of our recalibration mechanism, as it will be discussed in detail in the next section.

Note that, the density of the place field in recorded cells is influenced not only by the vigilance used for the Kohonen map but also by the size of the state centers. In scenarios where a recalibration area is notably large, the recalibration loop ensures the sustained activity of the PI field over this area, contributing to the creation of a large place field for the recruited cell.
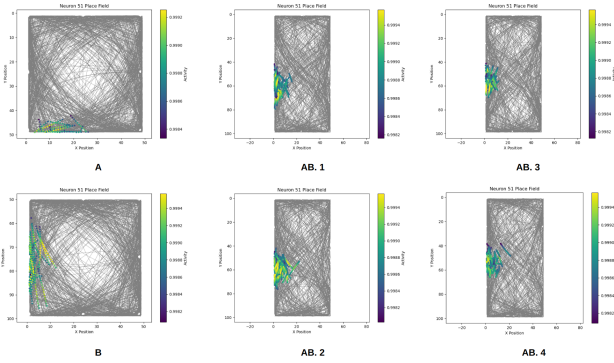
Fig. 6. The figure illustrates the place fields of PC 51 in room A (Figure A), room B (Figure B), and Room AB (Figures AB.1, AB.2, AB.3, and AB.4), where each figure corresponding to room AB represents, respectively, a non-overlapping 40000 time-step segment within the total 180000 time-step recording. The trajectory of the agent is given in gray.
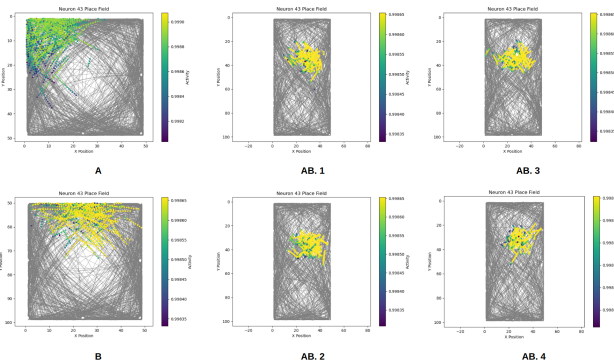
Fig. 7. The figure illustrates the place fields of PC 43 in room A (Figure A), room B (Figure B), and Room AB (Figures AB.1, AB.2, AB.3, and AB.4), where each figure corresponding to room AB represents, respectively, a non-overlapping 40000 time-step segment within the total 180000 time-step recording. The trajectory of the agent is given in gray.

V. LIMITATIONS

The limitation of our recalibration mechanism lies in the dynamic aspect resulting from different recalibration places. For instance, if the animal arrives in the center of a state with a PI containing accumulated errors, this can lead to memorizing incorrect recalibration directions from the PI, easily affecting the other recalibration directions imposed by the remaining state centers. Additionally, our recalibration mechanism is highly sensitive to the learning rate used for LMS1 during recalibration; with a high recalibration learning rate, if the recalibration direction learned previously for the state center is not precise enough, LMS1 quickly learns a biased PI, leading to a lack of stability. Conversely, with a small learning rate, recalibration could take a very long time to exhibit the averaging behavior of the predicted homing vectors.

Another inconvenience is that the animal can approach a state center without triggering recalibration for a sufficient time leading to an incomplete correction.

Our recalibration mechanism ensures stability within a very long time, but its effectiveness relies on the number of successful recalibrations. If a significant number of recalibration zones incorrectly adjust PI, it may cause other zones to shift their estimation of the "correct" PI to a point different from the origin.

VI. DISCUSSION AND PERSPECTIVES

Through the experiment, we observe that the model can generate activity similar to PCs. It is capable of maintaining a correct place code for subsequent iterations following updates to the environment. This observation indicates that the model tends to adapt to environmental changes.

As demonstrated in the theoretical explanation provided in the appendix, our model architecture aligns with the intended task. However, it exhibits certain limitations, primarily associated with the convergence time and the dynamic nature of recalibration directions between the recalibration zones. If not carefully controlled, these limitations may potentially propagate errors to PI.

An improvement can be achieved by controlling the impact of recalibration for each visually well-recognized area based on the frequency of the animal's visits. The more frequently an area is visited, the more significant the impact of the previously learned recalibration vector. This can be implemented by decreasing the learning rate of LMS2 each time the area is visited. Consequently, we gradually impose the old weights until reaching a low learning rate where stability is guaranteed. This approach can accelerate convergence and enhance the accuracy of our PI estimation. To enable this recalibration method to support environmental changes, it is essential not to entirely impose the learned recalibration. This ensures that PI has sufficient freedom to contribute and adapt gradually to the changes in the environment, until reaching a new place code configuration of the environment.

A robust recalibration mechanism, ensuring stability, can have a significant application in solving navigation problems in robotics, particularly in addressing the loop-closure detection challenge within SLAM algorithms. It is accurate in precisely locating the starting point without relying on vision every time. Besides, through the analysis of PC activity linked to specific

locations, the model effectively identifies when the robot returns to a past location, despite the changes occurring in the environment. This recognition becomes vital after extended exploration in unknown areas.

APPENDIX A
THEORETICAL EXPLANATION OF THE RECALIBRATION MECHANISM

The following learning rule is used to modify weights W_{ij} for the LMS algorithms in our model, such that $O_i(t) = W_{ij} \cdot C_j$, where λ corresponds to the learning rate and Δt is the time-step of a small movement of the animal:

$$\Delta W_{ij} = \lambda \cdot (U_i(t) - O_i(t)) \cdot C_j = W_{ij}(t + \Delta t) - W_{ij}(t) \quad (2)$$

After multiplying Eq. (2) by C_j:

$$\lambda \cdot (U_i(t) - O_i(t)) \cdot C_j^2 = O_i(t + \Delta t) - O_i(t) \quad (3)$$

Hence:

$$O_i(t + \Delta t) = (1 - \lambda \cdot C_j^2) \cdot O_i(t) + \lambda \cdot C_j^2 \cdot U_i(t) \quad (4)$$

For LMS1, Eq. (4) becomes Eq. (5), as we use a single constant context $C_0 = 1$. Outside a recalibration zone, $\lambda_{LMS_1} = 0.001$; thus Eq. (4), after replacing the values, becomes Eq. (5).

$$O_i^{\text{LMS}_1}(t + \Delta t) = 0.999 \cdot O_i^{\text{LMS}_1}(t) + 0.001 \cdot U_i(t) \quad (5)$$

Inside a recalibration zone LMS1 learns $U_i(t) = (O_i^{\text{LMS}_2}(t) + O_i^{\text{LMS}_1}(t))/2$, with a learning rate $\lambda_{LMS_1} = 0.1$; hence, Eq. (4) becomes Eq. (6).

$$O_i^{\text{LMS}_1}(t + \Delta t) = 0.9 \cdot O_i^{\text{LMS}_1}(t) + 0.1 \cdot U_i(t) \quad (6)$$

For LMS2, we use a learning rate $\lambda_{LMS_2} = 1$, corresponding to one-shot learning of LMS1. Learning takes place when the binary context is active; the context depends on whether the animal is inside a recalibration zone or not; $C_j = \mathbf{1}_{\text{state center}}$.

So when the agent is outside a recalibration zone, the weights are unchanged, and the output of LMS2 is null since the context is null.

$$O_i^{\text{LMS}_2}(t + \Delta t) = 0 \quad (7)$$

Inside a recalibration area, the learning of LMS1's output by LMS2 occurs with one time-step decay:

$$O_i^{\text{LMS}_2}(t + \Delta t) = O_i^{\text{LMS}_1}(t) \quad (8)$$

The recalibration equation of PI takes place for m consecutive iterations, is expressed as follows:

$$O_i^{\text{LMS}_1}(t + m \cdot \Delta t) = 0.9^m \cdot O_i^{\text{LMS}_1}(t) +$$
$$0.1 \cdot \sum_{n=0}^{m-1} (0.9^{m-1-n} \cdot U_i(t + n \cdot \Delta t)) \quad (9)$$

Below is the analysis of the two terms of this equation:
Term 1: $0.9^m \cdot O_i^{\textbf{LMS}_1}(t)$

This term represents an exponential decay factor that reduces the influence of the initial PI estimation $O_i^{\text{LMS}_1}(t)$ over time. As m increases, 0.9^m gets smaller, leading to a slow reduction in the impact of the initial position. This term provides memory in the recalibration process and allows the system to correct its estimation gradually.

Term 2: $0.1 \cdot \sum_{n=0}^{m-1} (0.9^{m-1-n} \cdot U_i(t + n \cdot \Delta t))$

This term accumulates contributions from U_i over m iterations. Each term in the sum, 0.9^{m-1-n}, decreases with time, giving less importance to older terms. This term aims to balance current information from $U_i(t)$ with historical information from previous iterations, which allows the recalibration process to consider both recent and previous adjustments achieved over the m iterations.

The recalibration equation combines an exponential decay factor 0.9^m for gradual adaptation to the new estimated PI, and a cumulative summation $\sum_{n=0}^{m-1} (0.9^{m-1-n} \cdot U_i(t + n \cdot \Delta t))$ as a balancing factor between currently learned homing vectors and the previously learned ones.

APPENDIX B
MODEL PARAMETERS

TABLE II
MODEL PARAMETERS IN ROOMS A AND B

Parameters	Outside recalibration	Inside recalibration
Learning rate (LMS1)	0.001	0.1
Learning rate (LMS2)	1	
Vigilance VPCs	0.86	
Vigilance PCs	0.996	
State center threshold	0.98	
Number of neurons in VPC field	600	
Number of neurons in PC field	100	

TABLE III
MODEL PARAMETERS IN ROOM AB

Parameters	Outside recalibration	Inside recalibration
Learning rate (LMS1)	0.001	0.1
Learning rate (LMS2)	1	
Vigilance VPCs	0	
Vigilance PCs	0	
State center threshold	0.91	
Number of neurons in VPC field	600	
Number of neurons in PC field	100	

The vigilance, ranging from 0 to 1, is used to regulate the number of learned cells. A higher vigilance leads to the recruitment of a larger number of cells, each with a narrow place field covering the environment. Conversely, a lower vigilance encodes a smaller number of PCs with wider place fields.

REFERENCES

[1] O'Keefe, J. & Dostrovsky, J. The hippocampus as a spatial map: preliminary evidence from unit activity in the freely-moving rat.. *Brain Research*. (1971)
[2] Save, E., Nerad, L. & Poucet, B. Contribution of multiple sensory information to place field stability in hippocampal place cells. *Hippocampus*. **10**, 64-76 (2000)

[3] Suzuki, S., Augerinos, G. & Black, A. Stimulus control of spatial behavior on the eight-arm maze in rats. *Learning And Motivation*. **11**, 1-18 (1980)

[4] Collett, T., Cartwright, B. & Smith, B. Landmark learning and visuo-spatial memories in gerbils. *Journal Of Comparative Physiology A*. **158** pp. 835-851 (1986)

[5] Mittelstaedt, H. & Mittelstaedt, M. Homing by path integration. *Avian Navigation*. pp. 290-297 (1982)

[6] Etienne, A. Navigation of a small mammal by dead reckoning and local cues. *Current Directions In Psychological Science*. **1**, 48-52 (1992)

[7] Knierim, J., Kudrimoti, H., Skaggs, W. & McNaughton, B. The interaction between vestibular cues and visual landmark learning in spatial navigation. *Perception, Memory, And Emotion: Frontiers In Neuroscience (Ono T, McNaughton B, Molotchnikoff S, Rolls E, Nishijo H, Eds)*. pp. 343-357 (1996)

[8] Goodridge, J. & Taube, J. Preferential use of the landmark navigational system by head direction cells in rats.. *Behavioral Neuroscience*. **109**, 49 (1995)

[9] Wiener, S., Korshunov, V., Garcia, R. & Berthoz, A. Inertial, substratal and landmark cue control of hippocampal CA1 place cell activity. *European Journal Of Neuroscience*. **7**, 2206-2219 (1995)

[10] Sharp, P., Blair, H., Etkin, D. & Tzanetos, D. Influences of vestibular and visual motion information on the spatial firing patterns of hippocampal place cells. *Journal Of Neuroscience*. **15**, 173-189 (1995)

[11] Darwin, C. Origin of certain instincts. *Nature*. **7**, 417-418 (1873)

[12] Alyan, S. & Jander, R. Short-range homing in the house mouse, Mus musculus: stages in the learning of directions. *Animal Behaviour*. **48**, 285-298 (1994)

[13] Colgin, L., Moser, E. & Moser, M. Understanding memory through hippocampal remapping. *Trends In Neurosciences*. **31**, 469-477 (2008)

[14] Latuske, P., Kornienko, O., Kohler, L. & Allen, K. Hippocampal remapping and its entorhinal origin. *Frontiers In Behavioral Neuroscience*. **11** pp. 253 (2018)

[15] Fyhn, M., Hafting, T., Treves, A., Moser, M. & Moser, E. Hippocampal remapping and grid realignment in entorhinal cortex. *Nature*. **446**, 190-194 (2007)

[16] Skaggs, W. & McNaughton, B. Spatial firing properties of hippocampal CA1 populations in an environment containing two visually identical regions. *Journal Of Neuroscience*. **18**, 8455-8466 (1998)

[17] Tanila, H. Hippocampal place cells can develop distinct representations of two visually identical environments. *Hippocampus*. **9**, 235-246 (1999)

[18] Gaussier, P. & Zrehen, S. Perac: A neural architecture to control artificial animals. *Robotics And Autonomous Systems*. **16**, 291-320 (1995)

[19] Ju, M. & Gaussier, P. A model of path integration and representation of spatial context in the retrosplenial cortex. *Biological Cybernetics*. **114**, 303-313 (2020)

[20] Gaussier, P., Banquet, J., Sargolini, F., Giovannangeli, C., Save, E. & Poucet, B. A model of grid cells involving extra hippocampal path integration, and the hippocampal loop. *Journal Of Integrative Neuroscience*. **6**, 447-476 (2007)

[21] Samsonovich, A. & McNaughton, B. Path integration and cognitive mapping in a continuous attractor neural network model. *Journal Of Neuroscience*. **17**, 5900-5920 (1997)

[22] Etienne, A., Maurer, R. & Séguinot, V. Path integration in mammals and its interaction with visual landmarks. *Journal Of Experimental Biology*. **199**, 201-209 (1996)

[23] Etienne, A. & Jeffery, K. Path integration in mammals. *Hippocampus*. **14**, 180-192 (2004)

[24] Knierim, J., Kudrimoti, H. & McNaughton, B. Interactions between idiothetic cues and external landmarks in the control of place cells and head direction cells. *Journal Of Neurophysiology*. **80**, 425-446 (1998)

[25] Agster, K. & Burwell, R. Hippocampal and subicular efferents and afferents of the perirhinal, postrhinal, and entorhinal cortices of the rat. *Behavioural Brain Research*. **254** pp. 50-64 (2013)

[26] Gaussier, P., Revel, A., Banquet, J. & Babeau, V. From view cells and place cells to cognitive map learning: processing stages of the hippocampal system. *Biological Cybernetics*. **86**, 15-28 (2002)

[27] Cuperlier, N., Quoy, M. & Gaussier, P. Neurobiologically inspired mobile robot navigation and planning. *Frontiers In Neurorobotics*. **1** pp. 104 (2007)

[28] Grossberg, S. & Grossberg, S. Contour enhancement, short term memory, and constancies in reverberating neural networks. *Studies Of Mind And Brain: Neural Principles Of Learning, Perception, Development, Cognition, And Motor Control*. pp. 332-378 (1982)

[29] Delarboulas, P., Gaussier, P., Quoy, M. & Caussy, R. Robustness study of a multimodal compass inspired form HD-cells and Dynamic neural fields. *SAB*. pp. 10-pages (2014)

[30] Jauffret, A., Cuperlier, N. & Gaussier, P. From grid cells and visual place cells to multimodal place cell: a new robotic architecture. *Frontiers In Neurorobotics*. **9** pp. 1 (2015)

[31] Widrow, B., Hoff, M. & Others Adaptive switching circuits. *IRE WESCON Convention Record*. **4**, 96-104 (1960)

[32] Lozano, Y., Page, H., Jacob, P., Lomi, E., Street, J. & Jeffery, K. Retrosplenial and postsubicular head direction cells compared during visual landmark discrimination. *Brain And Neuroscience Advances*. **1** pp. 2398212817721859 (2017)

[33] Wittmann, T. & Schwegler, H. Path integration—a network model. *Biological Cybernetics*. **73** pp. 569-575 (1995)

[34] Taube, J. Head direction cells and the neurophysiological basis for a sense of direction. *Progress In Neurobiology*. **55**, 225-256 (1998)

[35] Ju, M. Exploring the interaction between cortex and hippocampus to build spatial and visual grid cells: contributions to retrosplenial and entorhinal cortex modelling. (CY Cergy Paris Université,2023)

[36] Kohonen, T. The self-organizing map. *Proceedings Of The IEEE*. **78**, 1464-1480 (1990)

[37] Strösslin, T., Chavarriaga, R., Sheynikhovich, D. & Gerstner, W. Modelling path integrator recalibration using hippocampal place cells. *Artificial Neural Networks: Biological Inspirations–ICANN 2005: 15th International Conference, Warsaw, Poland, September 11-15, 2005. Proceedings, Part I 15*. pp. 51-56 (2005)

[38] Wernle, T., Waaga, T., Mørreaunet, M., Treves, A., Moser, M. & Moser, E. Integration of grid maps in merged environments. *Nature Neuroscience*. **21**, 92-101 (2018)

[39] Li, T., Arleo, A. & Sheynikhovich, D. Modeling place cells and grid cells in multi-compartment environments: entorhinal–hippocampal loop as a multisensory integration circuit. *Neural Networks*. **121** pp. 37-51 (2020)